Biomaterials Science

PAPER

View Article Online
View Journal | View Issue

Cite this: *Biomater. Sci.*, 2018, **6**, 1859

Tenascin-C derived signaling induces neuronal differentiation in a three-dimensional peptide nanofiber gel†

Melike Sever,‡[a] Gokhan Gunay,‡[b] Mustafa O. Guler *[c] and Ayse B. Tekinay *[a,b]

Received 19th September 2017,
Accepted 1st May 2018

DOI: 10.1039/c7bm00850c

rsc.li/biomaterials-science

The development of new biomaterials mimicking the neuronal extracellular matrix (ECM) requires signals for the induction of neuronal differentiation and regeneration. In addition to the biological and chemical cues, the physical properties of the ECM should also be considered while designing regenerative materials for nervous tissue. In this study, we investigated the influence of the microenvironment on tenascin-C signaling using 2D surfaces and 3D scaffolds generated by a peptide amphiphile nanofiber gel with a tenascin-C derived peptide epitope (VFDNFVLK). While tenascin-C mimetic PA nanofibers significantly increased the length and number of neurites produced by PC12 cells on 2D cell culture, more extensive neurite outgrowth was observed in the 3D gel environment. PC12 cells encapsulated within the 3D tenascin-C mimetic peptide nanofiber gel also exhibited significantly increased expression of neural markers compared to the cells on 2D surfaces. Our results emphasize the synergistic effects of the 3D conformation of peptide nanofibers along with the tenascin-C signaling and growth factors on the neuronal differentiation of PC12 cells, which may further provide more tissue-like morphology for therapeutic applications.

Introduction

Neural tissue engineering is a promising research field in regenerative medicine and aims to enhance the nerve regeneration process by understanding and mimicking the natural environment of neural cells through the use of bioactive scaffolds. The physical parameters of scaffolds are important in this context, as the materials to be used in tissue engineering must be able to mechanically and biologically support cells and allow the diffusion of oxygen, nutrients and growth factors.[2] Physical properties of the microenvironment are one of the most important aspects of regenerative materials and should be considered along the chemical and biological properties of the system when designing biomaterials for tissue engineering applications.[1] For *in vitro* studies, two-dimensional (2D) cell culture techniques are commonly used to study cell function and behavior, including cell attachment, proliferation, migration and differentiation, before the *in vivo* evaluation of the regenerative potential. However, while it is easy to control and manipulate the environment in 2D cell cultures, they are less compatible with *in vivo* systems and fail to mimic the native three-dimensional (3D) tissues. In contrast, 3D cultures are more accurate in representing the *in vivo* architecture of tissue environments since the cells within 3D culture systems can interact with each other in all dimensions.[2]

3D hydrogels and their cellular applications have been studied extensively, including Matrigel®, collagen, and alginate. Their structures are similar to the natural extracellular matrix, which strongly contributes to their bioactivity in regenerative medicine applications. However, these materials have some limitations including significant batch-to-batch variation and a lack of full range ECM-mimetic signals found in natural tissue environments.[3–5] Therefore, the use of synthetic biomaterials has significant potential for the development of an easy-to-use ECM-like environment and modifiable 3D culture systems.[6] Bioactive nanomaterials are particularly promising for the induction of neural differentiation and regeneration of

[a]*Institute of Materials Science and Nanotechnology, National Nanotechnology Research Center (UNAM), Bilkent University, Ankara 06800, Turkey. E-mail: mguler@uchicago.edu, atekinay@bilkent.edu.tr*
[b]*Neuroscience Graduate Program, Bilkent University, Ankara 06800, Turkey*
[c]*The Institute for Molecular Engineering, The University of Chicago, Chicago, IL 60637, USA*

†Electronic supplementary information (ESI) available: Liquid chromatography and mass spectrometry of peptide amphiphiles, *in vitro* experimental design, experimental groups, primers used for qRT-PCR expression analysis, gene expression analysis on day 3 and western blot analysis of ERK phosphorylation (p ERK) and total ERK expression. See DOI: 10.1039/c7bm00850c

‡These authors contributed equally.

nervous tissue, as they are able to provide biological, chemical and physical guidance to cells.[7,8] The extracellular matrix (ECM) is the non-cellular material that surrounds cells in tissue microenvironments and contains a wide range of proteins, proteoglycans, polysaccharides and signaling molecules, as well as water. Besides providing a physical support to cells, the ECM is fundamental in mediating the biochemical and biomechanical signaling mechanisms that occur between cells.[9] The development of bioactive materials that emulate the ECM of cells can therefore allow the precise manipulation of cellular behavior. Several short peptide sequences derived from ECM proteins have been used for neural cultures and demonstrated to induce neural differentiation. Among these, the laminin-derived Ile-Lys-Val-Ala-Val (IKVAV) and Tyr-Ile-Gly-Ser-Arg (YIGSR), as well as the fibronectin-derived Arg-Gly-Asp (RGD), are the most commonly used sequences to promote neural cell adhesion, migration and differentiation.[10–12] Biomaterials functionalized with these sequences were previously shown to be effective in promoting neural adhesion, proliferation and/or differentiation in *in vitro* studies.[13–17] Tenascins, which constitute an ECM glycoprotein family, have four family members: tenascin-C, tenascin-R, tenascin-W, and tenascin-Z. Among these types, tenascin-C has been extensively studied, and several studies showed that FN type III repeats of tenascin-C have a regulatory role in neurite outgrowth and guidance in rat cerebellar granule cells.[18–20] Tenascin-C is a multifunctional extracellular matrix glycoprotein that affects cell migration and neurite outgrowth when introduced into neuronal cell cultures *in vitro*.[21,22] It is expressed during the development of the central nervous system by glial cells and some neurons.[23] Tenascin-C was also shown to be involved in motor axon outgrowth[24] and play a role in spinal cord regeneration.[25] Meiners *et al.* showed that tenascin-C contains an eight-amino acid domain (VFDNFVLK) crucial for neurite extension,[26] and self-assembled scaffolds containing this sequence were recently shown to induce neurite outgrowth and migration in neural progenitor cells,[27] as well as to promote osteogenic differentiation in mesenchymal stem cells.[28] Also, the mechanism of action of tenascin-C on neurite outgrowth was determined which is mediated through the actions of integrin α7, α9, and β1.[29,30] All of these studies emphasize the central role of tenascin-C in the nervous system, and therefore we selected to mimic the tenascin-C protein to induce neuronal differentiation and neurite outgrowth in a 3D platform.

In this study, we investigated the stimulation of neuronal differentiation with a 3D peptide amphiphile nanofiber gel functionalized with a tenascin-C derived epitope (VFDNFVLK) and explored the influence of the culture microenvironment on this signal. The 3D cell culture system was found to provide both the biochemical and physical aspects of the native environment of neural cells, thereby filling the gap between 2D cell culture models and *in vivo* environments. Overall, we showed that 3D tenascin-C mimetic self-assembling nanofibers induced 3D neurite outgrowth and significantly increased the expressions of neural markers compared to 2D nanofiber and 3D epitope-free gel controls. This study features the cooperative effect of the culture dimensionality and bioactive signals for the induction of neuronal differentiation, which is critical for the design of neuroregenerative scaffolds. In addition, the 3D cell culture system described in this study can be used to facilitate the development of further organoid platforms.

Experimental section

Materials

All protected amino acids, lauric acid, 4-(2′,4′-dimethoxyphenyl-Fmoc-aminomethyl)-phenoxyacetamido-norleucyl-MBHA resin (Rink amide MBHA resin), 2-(1*H*-benzotriazol-1-yl)-1,1,3,3-tetramethyluroniumhexafluorophosphate (HBTU), and diisopropylethylamine (DIEA) were purchased from Nova-Biochem, ABCR, or Sigma-Aldrich. Cell culture materials were purchased from Invitrogen. All other chemicals and materials used in this study were purchased from Thermo Scientific or Sigma-Aldrich.

Synthesis and purification of peptide amphiphile (PA) molecules

PA molecules were synthesized on Rink Amide MBHA resin by using the Fmoc-protected solid phase peptide synthesis method. Amino acid couplings were performed with 2 equivalents of amino acids, which were activated with 1.95 equivalents of HBTU and 3 equivalents of DIEA for 2 h. Fmoc removal was performed with 20% piperidine–dimethylformamide (DMF) solution for 20 min. 10% acetic anhydride–DMF solution was used to permanently acetylate the unreacted amine groups after each coupling step. DMF and dichloromethane (DCM) were used as washing solvents after each step. The cleavage of the PAs and protection groups from the resin was carried out with a mixture of TFA : TIS : H_2O in the ratio of 95 : 2.5 : 2.5 for 3 h. Excess TFA removal was carried out by rotary evaporation. PAs in the remaining solution were precipitated in ice-cold diethyl ether overnight. The precipitate was collected by centrifugation the next day and dissolved in ultrapure water. This solution was frozen at −80 °C for 4 h and then lyophilized for 4–5 days. PAs were characterized by liquid chromatography-mass spectrometry (LC-MS). Mass spectra were obtained with an Agilent LC-MS equipped with an Agilent 6530 Q-TOF with an ESI source, using a Zorbax Extend-C18 2.1 × 50 mm column for basic conditions and a Zorbax SB-C8 4.6 × 100 mm column for acidic conditions. A gradient of water (0.1% formic acid or 0.1% NH_4OH) and acetonitrile (0.1% formic acid or 0.1% NH_4OH) was used for elution. In order to remove the residual TFA, positively-charged PAs were treated with 0.1 M HCl solution and lyophilized. To purify the peptides, an Agilent preparative reverse-phase HPLC system equipped with a Zorbax Extend-C18 21.2 × 150 mm column was used for basic conditions, and a Zorbax SB-C8 21.2 × 150 mm column was used for acidic conditions. A gradient of water (0.1% TFA or 0.1% NH_4OH) and acetonitrile (0.1% TFA or 0.1% NH_4OH) was used for the mobile phase. All peptides

were freeze-dried and reconstituted in ultrapure water at pH 7.4 before use.

Scanning electron microscopy (SEM) imaging of PA nanofibers

PA nanofiber networks were observed by SEM imaging. The oppositely charged PA solutions were mixed in equal volumes at a final volume of 30 μL to produce gels with neutral charges (12 mM TN–PA solution was mixed with 6 mM EE–PA solution, or 10 mM KK–PA solution was mixed with 10 mM EE–PA solution). Gels were formed on silicon wafers and dehydrated by sequential transfer to 20%, 40%, 60%, 80% and 100% v/v ethanol. Dehydrated gels were critical point-dried using a Tousimis Autosamdri 815B system. Dried PA gels were coated with 4 nm Au/Pd and SEM (FEI Quanta 200 FEG) images were obtained using an Everhart–Thornley Detector (ETD) in high vacuum mode at 5 keV beam energy.

Circular dichroism (CD)

A JASCO J815 CD spectrometer was used at room temperature for CD measurement. Oppositely charged 2.5×10^{-4} M PA solutions were mixed at appropriate volume ratios to a final volume of 300 μL (200 μL TN–PA solution was mixed with 100 μL EE–PA solution, or 150 μL KK–PA solution was mixed with 150 μL EE–PA solution) to produce nanofibers with net neutral charge. Measurements were carried out from 300 nm to 190 nm; the data interval and data pitch were 0.1 nm, and the scanning speed was 100 nm min^{-1}. All measurements were performed with three accumulations. The digital Integration Time (DIT) was selected as 1 s, the bandwidth as 1 nm, and the sensitivity was standard.

Oscillatory rheology

Oscillatory rheology measurements were performed with an Anton Paar Physica RM301 Rheometer operating with a 25 mm parallel plate configuration at 25 °C. Oppositely charged PA solutions with different concentrations were tested in order to optimize the stiffness of hydrogels according to the elastic properties of brain tissue. Different concentrations of each PA component, chosen to obtain neutral charges at a final volume of 250 μL, were carefully loaded onto the center of the lower plate and incubated for 10 min for gelation before measurement. After equilibration, the upper plate was lowered to a gap distance of 0.5 mm. Storage moduli (G') and loss moduli (G'') values were scanned from 100 rad s^{-1} to 0.1 rad s^{-1} of angular frequency, with a 0.5% shear strain. Three samples were measured for each PA gel.

Cell culture and maintenance

PC12 cells were used in all cell culture experiments. Cells were cultured in 25 cm^2 flasks at 37 °C in a humidified incubator and supplied with 5% CO_2. PC12 cells were maintained in Roswell Park Memorial Institute medium (RPMI) with 10% horse serum (HS), 5% fetal bovine serum (FBS), 2 mM L-glutamine and 1% penicillin/streptomycin (P/S). The culture medium was changed every 3 days.

3D cell cultures

For 3D gel formation, positively charged PA dissolved in 30 μL of 0.25 M sucrose and negatively charged PA dissolved in 30 μL of culture medium were placed into the wells to form a base layer (12 mM TN–PA solution was mixed with 6 mM EE–PA solution, or 10 mM KK–PA solution was mixed with 10 mM EE–PA solution). This gel was stabilized in a 37 °C incubator for 1 h. Then, the positively charged PA solution was placed onto this layer, and the negatively charged PA solution containing PC12 cells (5×10^5 cells per well) was added slowly with spiral motions. Gels were then placed into the incubator for 1 h for further stabilization. After 1 h, the medium was added to each well. The day after the gel formation, differentiation was induced with 20 ng mL^{-1} NGF treatment for the induction groups. The experiment was ended after 7 days of induction.

Flow cytometric analysis of viability

The viability of PC12 cells seeded on 2D or within 3D PA nanofibers was measured using the Annexin V-FITC Apoptosis Detection kit. After 24 h and 48 h of incubation, the flow cytometry protocol for Annexin V and propidium iodide was performed according to the manufacturer's instructions. Briefly, the medium was discarded; cells were washed with cold PBS and resuspended in 100 μL of 1× annexin-binding buffer, and 5 μL Alexa Fluor® 488 Annexin V and 1 μL of 100 μg mL^{-1} propidium iodide were added to each well. Cells were incubated at room temperature for 15 min and analyzed by flow cytometry, measuring the fluorescence emission at 530 nm (FL1 channel) and >575 nm (FL3 channel).

PC-12 neurite extension assay

Equal volumes of 4 mM TN–PA and 2 mM EE–PA were used to form gels with neutral charges in 6-well plates, while equal volumes of 3 mM KK–PA and EE–PA were mixed to form the epitope-free control PA group. PA-coated plates were incubated at 37 °C for 30 min prior to overnight incubation in a laminar flow hood at room temperature for solvent evaporation. The next day, PA matrices formed on 6-well plates were UV sterilized, and PC-12 cells (1.5×10^5 cells per well) were cultured on these matrices. Following the addition of cells in culture media to PA-coated surfaces, the PA matrix was rehydrated and formed a thin gel which adhered to the plate surface. RPMI with 10% HS, 5% FBS, 2 mM L-glutamine and 1% P/S was used as the culture medium. The day after seeding cells, media were changed with a neural induction medium consisting of MEM with 2% HS, 1% FBS, 2 mM L-glutamine, 1% P/S and 20 ng mL^{-1} NGF. A week after inducing cells with NGF, optical images were obtained at six random points of each well at 200× magnification. The total neurite length in each image was quantified by Image J and normalized by cell number/image. The average neurite length was obtained from six replicate wells for each coating material. In order to obtain another measure for the quantification of the neurite inducing potential of PA nanofibers, neurite extending cells were counted in the same images by Image J and the percentage of cells with

neurites was calculated. Cellular extensions spanning at least one cell body length were considered as neurites for quantification. The results were evaluated by one-way ANOVA for statistical significance.

SEM imaging of PC12 cells on 2D or within 3D PA nanofibers

The morphology and neurite extension pattern of PC12 cells were examined by SEM imaging using an ETD detector in high vacuum mode at 5 keV beam energy. Seven days after the incubation of PC12 cells on 2D or within 3D PA nanofibers, the cells were rinsed with PBS and fixed with 2% gluteraldehyde/PBS and 1 wt% OsO_4 for 1 h each. The fixed cells were washed with water, and then dehydrated sequentially in 20%, 40%, 60%, 80%, and 100% ethanol. The samples were critical point-dried with a Tousimis Autosamdri-815B system and coated with 6 nm Au–Pd before imaging.

Gene expression analysis

Gene expression profiles were assessed by quantitative RT-PCR analysis. Seven days after the incubation of PC12 cells on 2D or within 3D PA nanofibers, RNA was isolated using TRIzol (Invitrogen) according to the manufacturer's instructions. The yield and purity of the extracted RNA were assessed using a Nanodrop 2000 (Thermo Scientific). Primer sequences were designed using the NCBI database (Table S1, ESI†). cDNA synthesis from RNA and qRT-PCR were performed using a SuperScript III Platinum SYBR Green one-step qRT-PCR kit according to the manufacturer's instructions. Reaction conditions were briefly as follows: 55 °C for 5 min, 95 °C for 5 min, 40 cycles of 95 °C for 15 s, *X* °C for 30 s (varies according to primer sets), and 40 °C for 1 min, followed by a melting curve analysis to confirm product specificity. The reaction efficiencies for each primer set were evaluated by plotting a standard curve using 5-fold serial dilutions of total RNA. For analysis of the expression data, primary gene expression data were normalized by the expression level of GAPDH. A comparative Ct method (Pfaffl method) was used to analyze the results.

Western blot analysis

The total protein content of PC12 cells cultured under different conditions (2D or 3D culture, in the presence or absence of NGF) was isolated using TRIzol (Invitrogen) according to the manufacturer's instructions. Protein concentrations were determined using a BCA Protein Assay Kit (Thermo Scientific). Equal amounts of proteins (50 μg, 15 μL) were separated on 12% SDS-PAGE gels under denaturing and nonreducing conditions and then transferred to a PVDF membrane. The membrane was blocked with 5% nonfat milk in TBST at room temperature for 1 h and then incubated with βIII tubulin antibody (Abcam, ab78078, 1 : 1000), synaptophysin (Abcam, ab32127, 1 : 10 000), ERK 1/2 (Abcam, ab130004, 1 : 1000) and pERK (Abcam, ab50011, 1 : 1000) at 4 °C overnight. After washing in TBST, the blots were incubated with an HRP-conjugated secondary antibody (Millipore, 12-349 goat anti mouse IgG, 1 : 1000 or Abcam, ab6721 goat anti-rabbit IgG 1 : 2000). Signals were visualized using a chemiluminescent signal enhancement system (Invitrogen, Novex ECL). GAPDH was used as the internal control and treated with the same protocol (Millipore, MAB374, 1 : 1000). Gels were visualized by enhanced chemiluminescence (Bio-Rad) according to the manufacturer's protocol on a Bio-Rad ChemiDoc™ Imaging System with Image Lab™ Software, and protein concentrations in gel slabs were quantified using ImageJ. The intensities of the bands were normalized by GAPDH.

Statistical analysis

All quantitative values are presented as mean ± sem (standard error of means), and all the groups in the experiments were performed with at least three replicates. One-way analysis of variance (ANOVA) was used for statistical analysis, and *p*-values less than 0.05 were considered statistically significant.

Results and discussion

Design and characterization of peptide amphiphile nanofibers

Three-dimensional (3D) biomimetic nanofiber scaffolds have been used in biomedical tissue engineering due to their nanoscale architecture similar to the extracellular matrix found *in vivo*. These scaffolds are crucial for cellular organization and intercellular communication for regenerative purposes. However, the use of any such scaffold in the closed microenvironment of nerve tissue presents a critical challenge. Therefore, it is important to consider the required parameters carefully while designing a material for neuronal differentiation. In this work, we developed a 3D self-assembled nanofiber gel carrying a bioactive epitope derived from the natural extracellular matrix protein tenascin-C (lauryl-VFDNFVLKK-Am, TN–PA) and utilized it in order to fill the gap between 2D cell culture systems and *in vivo* tissue architectures. The potential of the tenascin-C mimetic peptide nanofiber system for promoting the neurite outgrowth was also studied. The control peptide amphiphiles, negatively charged EE–PA (lauryl-VVAGEE-Am) and positively charged KK–PA (lauryl-VVAGK-Am) lacked this epitope (Fig. 1). All PA molecules were synthesized by LC-MS and purified by preparative HPLC before use (Fig. S1†). Two nanofiber gels were used in this study: the TN–PA/EE–PA gel contained tenascin-C derived bioactive epitopes while the KK–PA/EE–PA gel was used as an epitope-free negative control. When positively charged PA molecules were mixed with negatively charged PA molecules, they formed ECM-mimetic nanofibers through self-assembly mediated by β-sheet driving motifs and electrostatic and hydrophobic interactions.[31] The SEM images revealed the nanofibrous and porous structure of peptide nanofiber gels, which resemble the networks formed by the natural extracellular matrix of cells at physiological pH (Fig. 2A). The secondary structures of the nanofibers were characterized by CD spectroscopy. Upon mixing the negatively and positively charged PA molecules, both bioactive and control nanofiber systems predominantly demonstrated the β-sheet structure with a

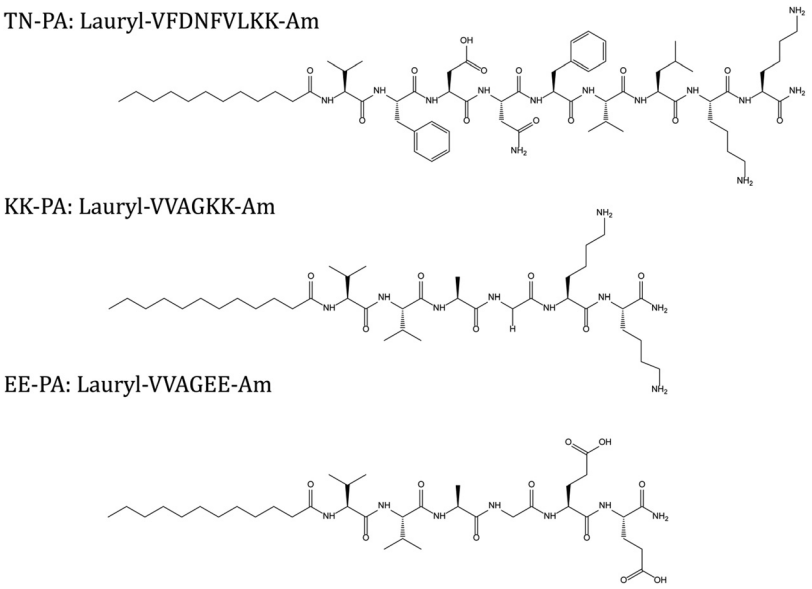

Fig. 1 Chemical structures of peptide amphiphile molecules.

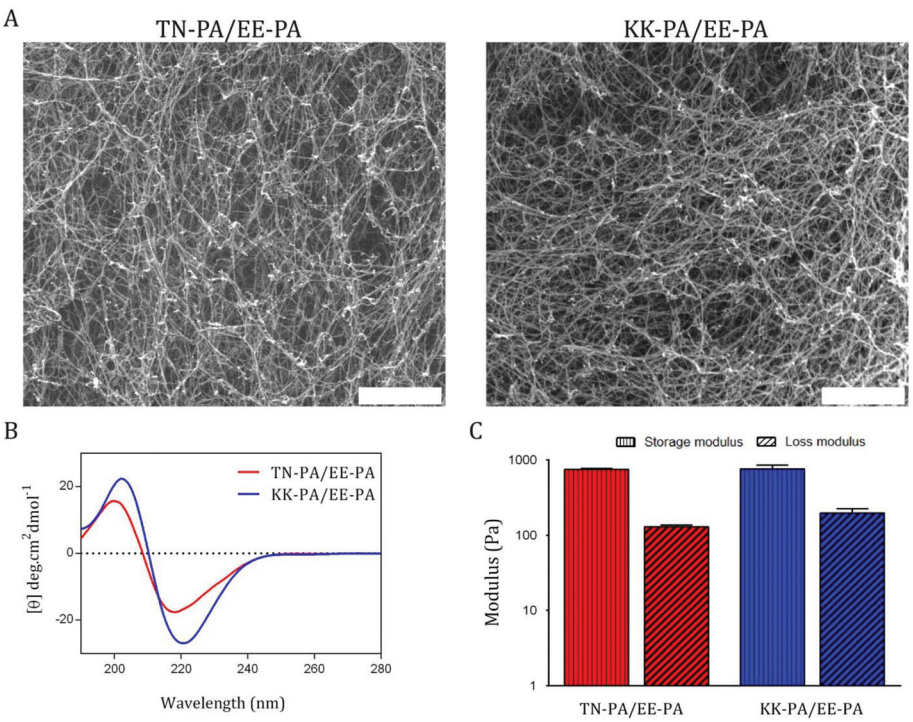

Fig. 2 SEM images of TN–PA/EE–PA and KK–PA/EE–PA (A), scale bars: 1 μm. CD spectra of TN–PA/EE–PA and KK–PA/EE–PA nanofibers (B). Equilibrium storage and loss modulus of TN–PA/EE–PA and KK–PA/EE–PA in water (C).

chiral absorbance maximum at around 200 nm and a minimum at around 220 nm (Fig. 2B).

The physical characteristics of the matrix are known to serve as potent cues for determining cell fates. When designing an artificial scaffold for neural cell culture, the mechanical properties of the scaffold should be optimized to resemble those of brain tissue, which has an elastic modulus of about 1 kPa.[32] Different concentrations of PA solutions were used to form neutral gels with mechanical properties close to the nervous system. Using frequency sweep rheology measurements at a constant strain, we performed oscillatory rheology analyses to assess the mechanical properties of peptide nanofiber gels. 12 mM TN–PA solution and 6 mM EE–PA solution (for the TN–PA/EE–PA combination) or 10 mM KK–PA solution

and 10 mM EE–PA solution (for the KK–PA/EE–PA combination) were used to form nanofiber gels with neutral charge at physiological pH. Both gel systems had a higher storage moduli (G') than loss moduli (G''), which indicates the gel-like structure of the system with approximately 1 kPa storage modulus at physiological pH (Fig. 2C).

Tenascin-C mimetic peptide nanofibers support cell viability

The cytotoxicity of regenerative materials under both *in vitro* and *in vivo* conditions is an important parameter that will determine their potential in clinical applications. Biomaterials used in tissue engineering applications should ideally not produce any toxic products or lead to any adverse reactions, which can be evaluated through *in vitro* cytotoxicity tests. In this study, the cellular viability of PC12 cells seeded on 2D or within 3D tenascin-C mimetic peptide nanofibers was assessed by flow cytometry analysis, by comparison with cells that were cultured on 2D or within 3D epitope-free peptide nanofibers at varying time points (24 and 48 h). Annexin V and propidium iodide were used to evaluate cellular survival, with the Annexin V^-/propidium $iodide^-$ population being considered as normal, healthy cells, the Annexin V^+/propidium $iodide^-$ population as cells at the early stages of apoptosis, and the Annexin V^+/propidium $iodide^+$ population as cells in late apoptosis. After 24 h and 48 h of incubation, the results showed that the percentages of live cells under all conditions were comparable to each other with no significant differences (Fig. 3). It is important to emphasize that the 3D scaffolds had the appropriate stiffness and porosity to support cell viability without diffusional transport limitations, which can limit the transfer of O_2 and other essential nutrients and cause the accumulation of toxic waste products within the scaffold space.

Tenascin-C mimetic peptide nanofibers promote neurite outgrowth

The ability to promote neurite outgrowth is crucial for neuroregenerative biomaterials since neurite development is required to generate functional synapses. PC12 is a rat adrenal gland pheochromocytoma-derived cell line that is commonly used as a model system in *in vitro* studies for the induction of differentiation in the presence of NGF.[33,34] Therefore, we used PC12 cells to evaluate the potential of tenascin-C mimetic peptide nanofibers to promote neurite extension, and measured the neurite lengths and the percentage of neurite-bearing cells on 2D TN–PA/EE–PA and KK–PA/EE–PA nanofibers. The neurite lengths measured at days 3 and 7 after the neural induction revealed that the TN–PA/EE–PA scaffold is a potent neurite inducer. The neurite extension on this scaffold was found to be significantly greater at both time points compared to the epitope-free KK–PA/EE–PA scaffold. In addition, the percentage of neurite-bearing cells on the tenascin-C mimetic scaffold was significantly higher compared to the control scaffold (Fig. 4).

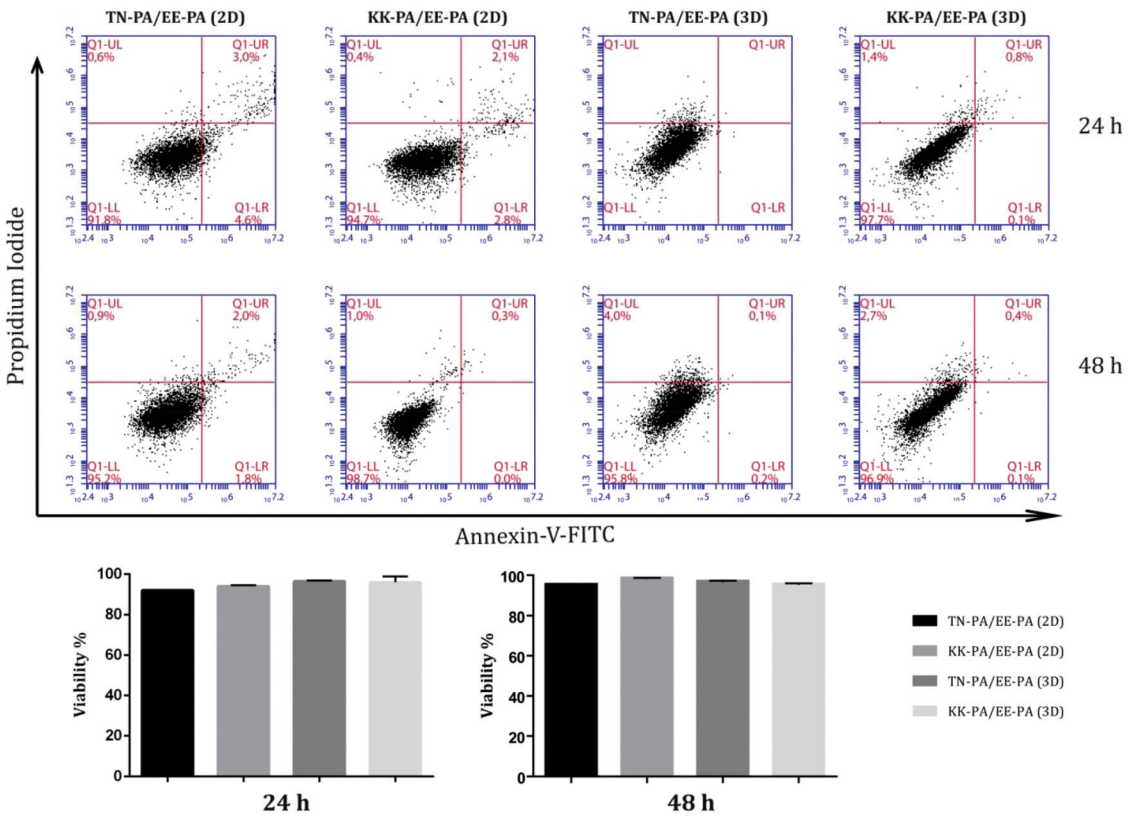

Fig. 3 Viability of PC12 cells seeded on 2D or within 3D peptide nanofibers which was tested by flow cytometry analysis. Values represent mean ± SD.

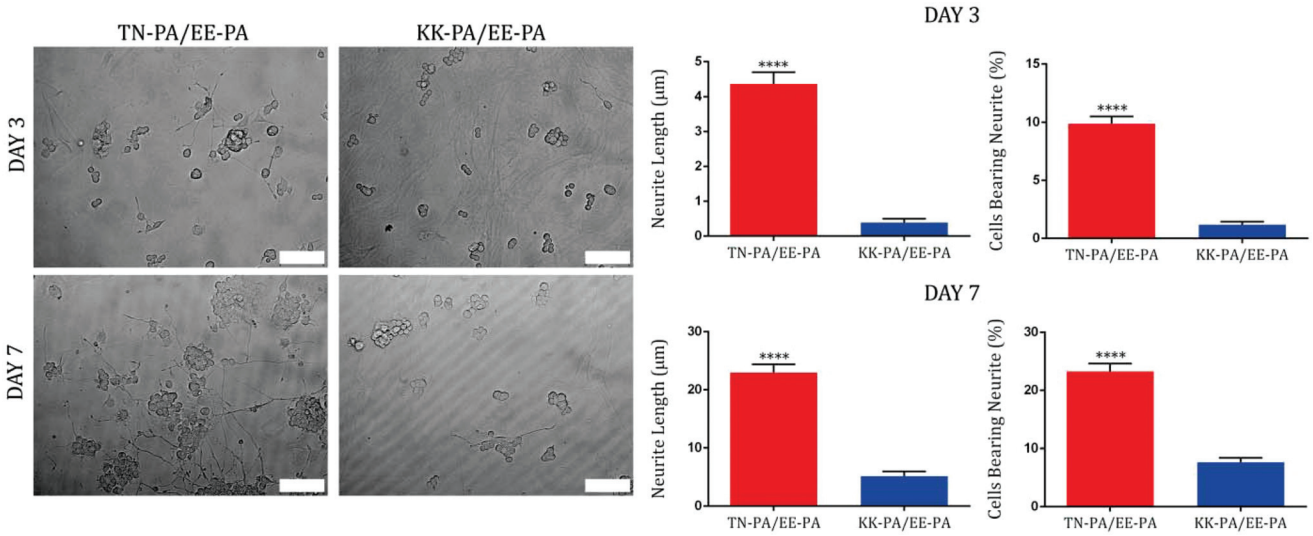

Fig. 4 Neurite outgrowth of PC-12 cells cultured on TN–PA/EE–PA and KK–PA/EE–PA nanofibers for 3 and 7 days, scale bars: 100 μm. Neurite length and percentage of neurite bearing cells were quantified for day 3 and day 7 by Image J. Values represent mean ± sem (***$p < 0.0001$).

Moreover, the neurite extension was promoted on the TN–PA/EE–PA scaffolds as early as 3 days, which further underlines the neurite outgrowth-promoting potential of tenascin-C derived signals in combination with NGF.

For 3D cell culture, we encapsulated PC12 cells within PA nanofibers in order to introduce tenascin-C signaling in all dimensions. 3D gels used in this study were composed of two layers. The first layer comprised a mixture of positively and negatively charged PA solutions, and the second layer included cells encapsulated within the PA mixture. Therefore, the cells encountered the first layer instead of the tissue culture plate when migrating downwards, and interacted with the tenascin-C derived epitope in three dimensions. The SEM images revealed that the encapsulation of PC12 cells within 3D nanofibers bearing tenascin-C derived epitopes induced neurite outgrowth in three dimensions, unlike 2D cell culture conditions in which neurite extension was only in two dimensions (Fig. 5).

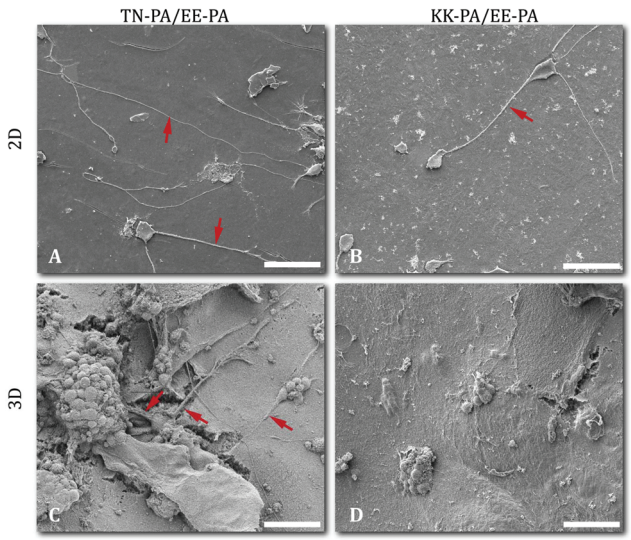

Fig. 5 SEM images of PC-12 cells cultured on 2D TN–PA/EE–PA, EE–PA/KK–PA nanofibers, and 3D TN–PA/EE–PA, EE–PA/KK–PA gels on day 7 after cell seeding. Scale bars are 50 μm.

Tenascin-C mimetic peptide nanofibers enhance neural gene expressions

The gene expression profiles of PC12 cells cultured on 2D or within 3D bioactive or non-bioactive nanofibers were analyzed to understand the effect of the tenascin-C derived epitope on neuronal differentiation. Gene expressions of β-III tubulin and synaptophysin I under different conditions were determined as indicators of neuronal differentiation. β-III tubulin is a widely used marker for neuronal differentiation, since it is expressed in both mature and immature neurons.[35,36] The encapsulation of PC12 cells within 3D tenascin-C mimetic peptide nanofibers increased the gene expression of βIII-tubulin in the presence of NGF when compared to other groups (Fig. 6A).

Synaptophysin is a commonly used neuronal differentiation marker and presynaptic vesicle protein that is present in axons, expressed throughout the brain and responsible for synapse formation.[37,38] The results of the synaptophysin expression analysis displayed a similar pattern to βIII-tubulin expression. In the presence of NGF, the tenascin-C epitope significantly increased the gene expression of synaptophysin when the cells were encapsulated within the 3D nanofiber gel. Strikingly, when the cells were encapsulated within 3D tenascin-C mimetic nanofibers in the absence of NGF, synaptophysin expression was enhanced to a greater extent compared to 2D culture conditions, suggesting that the 3D introduction of tenascin-C signaling to cells is more effective for inducing synaptophysin expression compared to its 2D counterpart (Fig. 6A). However, when the neural gene expressions of PC12 cells cultured on 2D or within 3D epitope-free control nano-

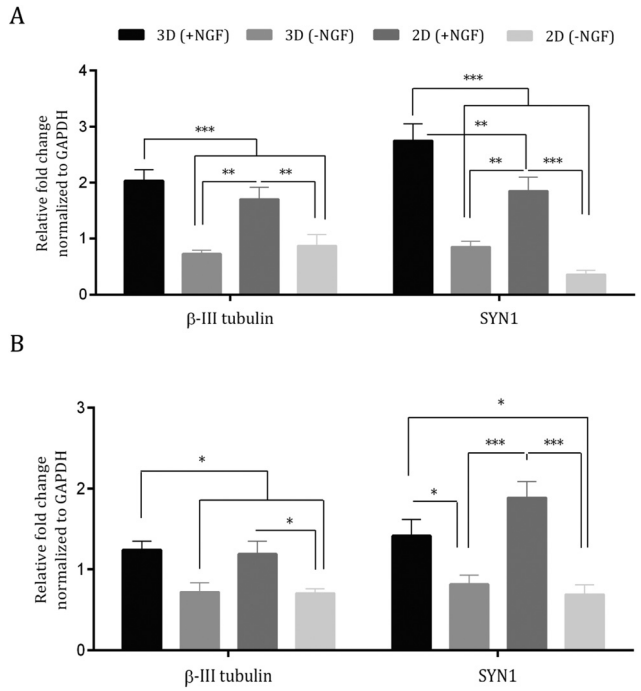

Fig. 6 Gene expression analyses of β-III tubulin and Synaptophysin I (SYN1) on day 7 on 2D nanofibers and in 3D hydrogels with and without the addition of NGF. Gene expression levels of PC-12 cells cultured on TN–PA/EE–PA nanofibers and hydrogels (A). Gene expression levels of PC-12 cells on KK–PA/EE–PA nanofibers and hydrogels (B). Expression level of each gene was normalized to GAPDH. Values represent mean ± sem (***$p < 0.001$, **$p < 0.01$, *$p < 0.05$).

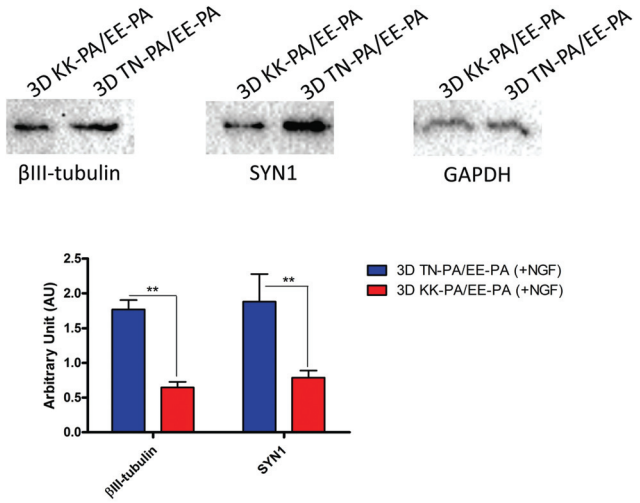

Fig. 7 Western blot analysis for βIII-tubulin and SYN1 protein expression of PC12 cells seeded in 3D TN–PA/EE–PA or KK–PA/EE–PA hydrogels with NGF induction. Values represent mean ± sem (**$p < 0.01$).

fiber gels were analyzed, the presence or absence of NGF did not correlate with the microenvironment, suggesting that the bioactivity and microenvironment cooperate for neuronal differentiation (Fig. 6B). Overall, these results confirm the SEM results showing extensive neurite outgrowth of PC12 cells encapsulated within 3D tenascin-C mimetic nanofibers.

Tenascin-C mimetic peptide nanofibers enhance neural protein expression

For further analysis of the neuronal differentiation potential of PC12 cells with tenascin-C signaling and 3D cell culture, protein expression levels of neural markers were quantified by western blotting. Protein-level analysis revealed the increased expression of synaptophysin and βIII-tubulin proteins in PC12 cells concomitantly with enhanced neuronal differentiation induced by tenascin-C signaling in the 3D nanofiber system compared to epitope-free 3D nanofibers (Fig. 7). Our results suggest that introducing tenascin-C signals in three dimensions not only increased the expression levels of neural markers at the gene level, but also maintained the translation of gene upregulation to the protein level.

We further confirmed neuronal differentiation as a result of the synergy between tenascin-C signaling and the 3D gel system by evaluating the activation of the ERK 1/2 module, since ERK1/2 is strongly activated by growth factors such as NGF,[39] which was used in our study. We found that there was no statistically significant difference between the [phospho ERK 1/2]/[total ERK 1/2] ratio of cells seeded within 3D bioactive and non-bioactive gels (Fig. S5†). Consequently, the effect of NGF is the same for both 3D conditions (bioactive or non-bioactive), and the neuronal differentiation induction effect in the tenascin-C mimetic 3D gel only comes from the action of tenascin-C signaling in the context of a 3D microenvironment.

Conclusion

We have shown that 3D peptide nanofibers with favorable mechanical and biochemical properties are able to support the neuronal differentiation with extensive neurite outgrowth and regulation of neural markers. The tenascin-C derived signal containing nanofibers promoted significant neurite extension, which was further stimulated by the 3D nanofiber scaffolds because the cells face bioactive signals from all directions. On the other hand, the cells had contact with only a portion of the bioactive signals on the 2D nanofiber scaffolds. The ability to combine the physical and biochemical properties of the peptide amphiphile nanofibers in one system presents more tissue-like platforms for the development of new therapies for neurological conditions and disorders.

Author contributions

The manuscript was written through the contribution of all authors. All authors have given approval to the final version of the manuscript.

Conflicts of interest

The authors declare no competing financial interest.

Acknowledgements

We thank Z. Erdogan and M. Guler for their technical help in the purification and characterization of PA nanofibers. M. S. is supported by the TUBITAK-BIDEB (2211) Ph.D. fellowship, and G. G. is supported by the TUBITAK-BIDEB (2210-C) M.Sc. fellowship. A. B. T. acknowledges the support from the Science Academy Outstanding Young Scientist Award (BAGEP).

References

1 M. Sever, B. Mammadov, M. Gecer, M. O. Guler and A. B. Tekinay, Nanomaterials for Neural Regeneration, *Ther. Nanomater.*, 2016, 33.
2 M. C. LaPlaca, V. N. Vernekar, J. T. Shoemaker and D. K. Cullen, Three-dimensional neuronal cultures, in *Methods in bioengineering: 3D tissue engineering*, Artech House, Norwood, MA, 2010, pp. 187–204.
3 N. C. Hunt, D. Hallam, A. Karimi, C. B. Mellough, J. Chen, D. H. W. Steel and M. Lako, 3D culture of human pluripotent stem cells in RGD-alginate hydrogel improves retinal tissue development, *Acta Biomater.*, 2017, **49**, 329–343.
4 M. N. Labour, A. Banc, A. Tourrette, F. Cunin, J. M. Verdier, J. M. Devoisselle, A. Marcilhac and E. Belamie, Thick collagen-based 3D matrices including growth factors to induce neurite outgrowth, *Acta Biomater.*, 2012, **8**(9), 3302–3312.
5 K. Y. Lee and D. J. Mooney, Alginate: properties and biomedical applications, *Prog. Polym. Sci.*, 2012, **37**(1), 106–126.
6 G. Gunay, M. Sever, A. B. Tekinay and M. O. Guler, Three-Dimensional Laminin Mimetic Peptide Nanofiber Gels for In Vitro Neural Differentiation, *Biotechnol. J.*, 2017, **12**(12), DOI: 10.1002/biot.201700080.
7 C. E. Schmidt and J. B. Leach, Neural tissue engineering: strategies for repair and regeneration, *Annu. Rev. Biomed. Eng.*, 2003, **5**, 293–347.
8 M. Sever, I. Uyan, A. B. Tekinay and M. O. Guler, Bioactive Nanomaterials for Neural Engineering, in *Neural Engineering*, Springer, 2016, pp. 181–206.
9 C. Frantz, K. M. Stewart and V. M. Weaver, The extracellular matrix at a glance, *J. Cell Sci.*, 2010, **123**(24), 4195–4200.
10 J. Graf, R. C. Ogle, F. A. Robey, M. Sasaki, G. R. Martin, Y. Yamada and H. K. Kleinman, A pentapeptide from the laminin B1 chain mediates cell adhesion and binds the 67,000 laminin receptor, *Biochemistry*, 1987, **26**(22), 6896–6900.
11 M. D. Pierschbacher and E. Ruoslahti, Cell attachment activity of fibronectin can be duplicated by small synthetic fragments of the molecule, *Nature*, 1984, **309**(5963), 30–33.
12 K. Tashiro, G. C. Sephel, B. Weeks, M. Sasaki, G. R. Martin, H. K. Kleinman and Y. Yamada, A synthetic peptide containing the IKVAV sequence from the A chain of laminin mediates cell attachment, migration, and neurite outgrowth, *J. Biol. Chem.*, 1989, **264**(27), 16174–16182.
13 G. A. Silva, C. Czeisler, K. L. Niece, E. Beniash, D. A. Harrington, J. A. Kessler and S. I. Stupp, Selective differentiation of neural progenitor cells by high-epitope density nanofibers, *Science*, 2004, **303**(5662), 1352–1355.
14 B. Ananthanarayanan, L. Little, D. V. Schaffer, K. E. Healy and M. Tirrell, Neural stem cell adhesion and proliferation on phospholipid bilayers functionalized with RGD peptides, *Biomaterials*, 2010, **31**(33), 8706–8715.
15 T. T. Yu and M. S. Shoichet, Guided cell adhesion and outgrowth in peptide-modified channels for neural tissue engineering, *Biomaterials*, 2005, **26**(13), 1507–1514.
16 J. C. Schense, J. Bloch, P. Aebischer and J. A. Hubbell, Enzymatic incorporation of bioactive peptides into fibrin matrices enhances neurite extension, *Nat. Biotechnol.*, 2000, **18**(4), 415–419.
17 B. Mammadov, R. Mammadov, M. O. Guler and A. B. Tekinay, Cooperative effect of heparan sulfate and laminin mimetic peptide nanofibers on the promotion of neurite outgrowth, *Acta Biomater.*, 2012, **8**(6), 2077–2086.
18 S. Meiners and H. M. Geller, Long and short splice variants of human tenascin differentially regulate neurite outgrowth, *Mol. Cell. Neurosci.*, 1997, **10**(1–2), 100–116.
19 S. Meiners, M. L. Mercado, M. S. Nur-e-Kamal and H. M. Geller, Tenascin-C contains domains that independently regulate neurite outgrowth and neurite guidance, *J. Neurosci.*, 1999, **19**(19), 8443–8453.
20 S. Meiners, E. M. Powell and H. M. Geller, Neurite outgrowth promotion by the alternatively spliced region of tenascin-C is influenced by cell-type specific binding, *Matrix Biol.*, 1999, **18**(1), 75–87.
21 K. Husmann, S. Carbonetto and M. Schachner, Distinct sites on tenascin-C mediate repellent or adhesive interactions with different neuronal cell types, *Cell Adhes. Commun.*, 1995, **3**(4), 293–310.
22 K. Husmann, A. Faissner and M. Schachner, Tenascin promotes cerebellar granule cell migration and neurite outgrowth by different domains in the fibronectin type III repeats, *J. Cell Biol.*, 1992, **116**(6), 1475–1486.
23 Y. Zhang, P. N. Anderson, G. Campbell, H. Mohajeri, M. Schachner and A. R. Lieberman, Tenascin-C expression by neurons and glial cells in the rat spinal cord: changes during postnatal development and after dorsal root or sciatic nerve injury, *J. Neurocytol.*, 1995, **24**(8), 585–601.
24 J. Schweitzer, T. Becker, J. Lefebvre, M. Granato, M. Schachner and C. G. Becker, Tenascin-C is involved in motor axon outgrowth in the trunk of developing zebrafish, *Dev. Dyn.*, 2005, **234**(3), 550–566.
25 Y. M. Yu, M. Cristofanilli, A. Valiveti, L. Ma, M. Yoo, F. Morellini and M. Schachner, The extracellular matrix glycoprotein tenascin-C promotes locomotor recovery after

spinal cord injury in adult zebrafish, *Neuroscience*, 2011, **183**, 238–250.

26 S. Meiners, M. S. A. Nur-E-Kamal and M. L. T. Mercado, Identification of a neurite outgrowth-promoting motif within the alternatively spliced region of human tenascin-C, *J. Neurosci.*, 2001, **21**(18), 7215–7225.

27 E. J. Berns, Z. Alvarez, J. E. Goldberger, J. Boekhoven, J. A. Kessler, H. G. Kuhn and S. I. Stupp, A tenascin-C mimetic peptide amphiphile nanofiber gel promotes neurite outgrowth and cell migration of neurosphere-derived cells, *Acta Biomater.*, 2016, **37**, 50–58.

28 M. Sever, B. Mammadov, M. O. Guler and A. B. Tekinay, Tenascin-C mimetic Peptide nanofibers direct stem cell differentiation to osteogenic lineage, *Biomacromolecules*, 2014, **15**(12), 4480–4487.

29 M. L. Mercado, A. Nur-e-Kamal, H. Y. Liu, S. R. Gross, R. Movahed and S. Meiners, Neurite outgrowth by the alternatively spliced region of human tenascin-C is mediated by neuronal alpha7beta1 integrin, *J. Neurosci.*, 2004, **24**(1), 238–247.

30 M. R. Andrews, S. Czvitkovich, E. Dassie, C. F. Vogelaar, A. Faissner, B. Blits, F. H. Gage, C. ffrench-Constant and J. W. Fawcett, Alpha9 integrin promotes neurite outgrowth on tenascin-C and enhances sensory axon regeneration, *J. Neurosci.*, 2009, **29**(17), 5546–5557.

31 K. L. Niece, J. D. Hartgerink, J. J. J. M. Donners and S. I. Stupp, Self-assembly combining two bioactive peptide-amphiphile molecules into nanofibers by electrostatic attraction, *J. Am. Chem. Soc.*, 2003, **125**(24), 7146–7147.

32 P. C. Georges, W. J. Miller, D. F. Meaney, E. S. Sawyer and P. A. Janmey, Matrices with compliance comparable to that of brain tissue select neuronal over glial growth in mixed cortical cultures, *Biophys. J.*, 2006, **90**(8), 3012–3018.

33 L. A. Greene and A. S. Tischler, Establishment of a noradrenergic clonal line of rat adrenal pheochromocytoma cells which respond to nerve growth factor, *Proc. Natl. Acad. Sci. U. S. A.*, 1976, **73**(7), 2424–2428.

34 D. Vaudry, P. J. Stork, P. Lazarovici and L. E. Eiden, Signaling pathways for PC12 cell differentiation: making the right connections, *Science*, 2002, **296**(5573), 1648–1649.

35 M. K. Lee, J. B. Tuttle, L. I. Rebhun, D. W. Cleveland and A. Frankfurter, The expression and posttranslational modification of a neuron-specific beta-tubulin isotype during chick embryogenesis, *Cell Motil. Cytoskeleton*, 1990, **17**(2), 118–132.

36 J. R. Menezes and M. B. Luskin, Expression of neuron-specific tubulin defines a novel population in the proliferative layers of the developing telencephalon, *J. Neurosci.*, 1994, **14**(9), 5399–5416.

37 E. M. Fykse, K. Takei, C. Walch-Solimena, M. Geppert, R. Jahn, P. De Camilli and T. C. Sudhof, Relative properties and localizations of synaptic vesicle protein isoforms: the case of the synaptophysins, *J. Neurosci.*, 1993, **13**(11), 4997–5007.

38 B. Marqueze-Pouey, W. Wisden, M. L. Malosio and H. Betz, Differential expression of synaptophysin and synaptoporin mRNAs in the postnatal rat central nervous system, *J. Neurosci.*, 1991, **11**(11), 3388–3397.

39 T. S. Lewis, P. S. Shapiro and N. G. Ahn, Signal transduction through MAP kinase cascades, *Adv. Cancer Res.*, 1998, **74**, 49–139.

